ceramics

MDPI

Article

Physical and Mechanical Properties of Fired Bricks from Amazon Bauxite Tailings with Granite Powder

Igor A. R. Barreto * and Marcondes L. da Costa *

Program for Post-Graduation in Geology and Geochemistry, Institute of Geosciences, Federal University of Pará Belém, Belém 66075-110, PA, Brazil

* Correspondence: igorrochaq@gmail.com (I.A.R.B.); marcondeslc@gmail.com (M.L.d.C.)

Abstract: In the Amazon region, bauxite processing generates significant quantities of clay mineral-rich tailings, which pose a major challenge for bauxite mining operations. This study explores the use of bauxite tailings to produce fired bricks and evaluates their properties. Using a Box–Behnken experimental design, nine specimens were prepared with varying granite content (0%, 5%, 10%, 20%, and 30%) and fired at three different temperatures: 800 °C, 900 °C, and 1000 °C. The bauxite tailings contain gibbsite, kaolinite, Al-goethite, and hematite, while the granite powder comprises quartz, potassium feldspar, sodium plagioclase, muscovite, and occasionally kaolinite. Linear shrinkage values remained within recommended limits, below 8%. Apparent porosity (AP) results ranged from 60.2% to 72%, with maximum water absorption reaching 23.6%. The compressive strength of bricks without granite addition was 11.9 MPa at 900 °C, with the highest value recorded at 14.9 MPa at 800 °C when granite was added. These findings indicate that bauxite tailings, when supplemented with pulverized granite, exhibit promising potential for fired brick production.

Keywords: mining tailings; ceramics; kaolinite; circular economy

Academic Editors: Francesco Baino, Pardeep Gianchandani, Enrico Fabrizio, Bartolomeo Megna and Manuela Ceraulo

Received: 14 March 2025
Revised: 11 April 2025
Accepted: 11 April 2025
Published: 13 April 2025

Citation: Barreto, I.A.R.; da Costa, M.L. Physical and Mechanical Properties of Fired Bricks from Amazon Bauxite Tailings with Granite Powder. *Ceramics* **2025**, *8*, 37. https://doi.org/10.3390/ceramics8020037

1. Introduction

The red ceramics sector is still an important source of essential materials for the construction industry and other sectors [1–6]. Red ceramics include blocks, roof tiles, solid bricks (fired bricks), drainage pipes, slabs, green walls, hollow elements, and expanded clay [7]. The term red ceramic is applied to these materials because of the red coloration that appears during firing and remains afterward, conferred by the newly formed minerals such as hematite (Fe_2O_3) and maghemite [7]. The raw materials used to produce red ceramics generally come from natural sources (rocks and soils), industrial waste, and even synthetic materials.

Clay is fundamental in the raw material used to produce red ceramics. It consists mainly of illite and kaolinite, with restricted montmorillonite, among others, which are responsible for the property of "plasticity" when it is mixed with water, which facilitates its handling in the shaping of different types of ceramic pieces and their various applications [1,3]. Certain clay minerals contribute to the plasticity of a ceramic piece and play other roles. For instance, illite, which contains K_2O in its composition, acts as a flux during the firing process [3].

A material used in the production of ceramics is unlikely to consist solely of clay minerals, even when it originates from natural sources. Such materials typically contain a variety of other constituents, including minerals like muscovite, goethite, hematite, quartz, and anatase, as well as organic matter and even sulfides such as pyrite. These components

significantly influence the properties of the ceramic material, either positively or negatively. For instance, minerals such as quartz and anatase impart a non-plastic character to the ceramic body, whereas goethite, hematite, and muscovite can act as fluxing agents during the firing process, enhancing the mechanical strength of the final product [3]. The presence of organic matter is not desirable, as it can cause pores to form inside the ceramic piece, reducing its strength.

The material used to produce red ceramics does not always contain all the essential minerals to achieve the properties needed to produce high-quality ceramics, meaning that two or more raw materials must be mixed in pre-defined proportions to obtain a product with the right properties. Similar technological products are only suitable for specific applications if their raw materials possess distinct characteristics, often achieved through the use of additives. For instance, materials like Markforged 17-4 PH and BASF Ultrafuse 316L enable the production of stainless steel, while fibers enhance composite materials. Additionally, Artificial Intelligence can optimize material compositions and processing parameters to achieve target properties. In the production of biodegradable or recyclable polymers, biomass serves as a sustainable raw material. Numerous applications require specific additives to ensure the materials meet performance standards and achieve desirable properties [8–13].

In Paragominas, Pará, Brazil, the company Mineração Paragominas S.A. extracts and processes bauxite from regional deposits as a raw material for the production of metallic aluminum in Barcarena, Pará. During the bauxite beneficiation process—which includes crushing, grinding, and washing—a significant amount of clay-rich material is generated and mixed with water. For every ton of bauxite ore processed, approximately 0.35 tons of this clay residue are produced. Until recently, this by-product was disposed of in tailings basins.

The tailing consists mainly of kaolinite (the predominant mineral), gibbsite, hematite, goethite, quartz, and anatase. This mineralogical composition, which is dominated by clay, combined with the fact that it is available in large volumes in the tailing's ponds and previous laboratory research, demonstrates the very attractive potential of this waste for applications in civil construction, such as bricks, cement, and mortar, among others [14]. Despite these aspects, this material currently has no applications and could be considered a potential problematic waste for bauxite mining.

Because of the points listed above, this study aims to assess the technical feasibility of producing "burnt brick" from these clay residues from bauxite mining in Paragominas, with and without the addition of pulverized granite. The choice of granite powder is intended to demonstrate the potential of fine waste resulting from the production of gravel from these rocks in quarries in the region.

2. Materials and Methods

2.1. Raw Materials

The raw material used in the development of this study consisted of a representative sample of bauxite tailing (ALB-1) from the Mineração Paragominas S.A company of Paragominas Pará, PA, Brazil. Additionally, pulverized granite (GP-1) from a quarry in the region was used as an additive.

2.2. The Characterization of the Samples

2.2.1. Mineralogical Composition

The mineralogical phases of the sample were determined using X-ray diffraction (XRD) in accordance with the powder method. A BRUKER diffractometer, model D2 PHASER, equipped with a θ/θ goniometer, a radius of 141.1 nm, and a copper anode emitting

at a characteristic wavelength of 1.54 Å (8.047 keV, Cu-Kα1) was utilized, operating at a maximum power of 300 W (30 kV × 10 mA). A linear Lynxeye detector with a 5° 2θ aperture and 192 channels was employed for data collection. The analyses were conducted at the Laboratory of Mineralogy, Geochemistry, and Applications (LAMIGA-UFPA) within the Institute of Geosciences at the Federal University of Pará (UFPA).

2.2.2. Chemical Composition with X-Ray Fluorescence Spectrometry

The major chemical elements were determined using X-ray fluorescence spectrometry (XRF) through the preparation of a fused pellet. The pellet was prepared with a sample-to-flux ratio (lithium tetraborate) established according to the XRF79C_10 method. Analyses were conducted at the Chemical Analysis Laboratory of SGS GEOSOL, located in Vespasiano, Minas Gerais, Brazil.

The loss on ignition (LOI) was determined using the gravimetric method, involving the calcination of previously dried samples at 1000 °C.

2.2.3. Thermogravimetric Analysis (TGA) and Differential Scanning Calorimetry (DSC)

Thermogravimetric and differential scanning calorimetry (TGA/DSC) analyses were conducted using a NETZSCH model STA 449 F5 Jupiter, which features a simultaneous thermal analyzer equipped with a vertical cylindrical oven. The analyses were performed under a nitrogen flow rate of 50 mL/s, a heating rate of 10 °C/min, and a temperature range from 30 °C to 1100 °C. This procedure was carried out at the Laboratory of Mineralogy, Geochemistry, and Applications (LAMIGA-UFPA) within the Institute of Geosciences at the Federal University of Pará (UFPA).

2.3. Formulation and Characterization of Fired Brick

The bauxite tailing (ALB-1) and granite (GP-1) samples were initially dried at 110 °C for 24 h. Subsequently, the granite sample underwent a preparation process that included crushing, grinding, and sieving through an 80-mesh sieve to produce a uniform powder. The ALB-1 sample, however, did not undergo particle size reduction. For the formulation of test specimens, both samples were combined in various weight ratios (wt%), ranging from 0 to 30% granite powder and 70 to 100% ALB-1, to achieve a final mass of 30 g (Table 1). This blend of ALB-1 and GP-1 was then transferred to a porcelain dish, where 10% water (g/g) was added and the mixture was homogenized using a pestle for 5 min.

Table 1. Experimental matrix and real and coded values of the independent variables.

Experiment	Temperature (°C)	Percentage of Granite Powder (wt/wt)
C1	1000	20
C2	1000	5
C3	900	0
C4	800	5
C5	800	20
C6	900	30
C7	900	10
C8	900	10
C9	900	10

The prepared mass was then used to form test specimens (CPs) in steel molds shaped as parallelepipeds with dimensions of 50.0 mm × 20.0 mm × 10.0 mm. Specimen compaction was performed via single-action uniaxial pressing at 30 kgf/cm^2 using a hydraulic press

(Karl Kolb, model PW-40). Following pressing, the specimens were dried at 105 °C for 24 h and subsequently fired at varying final temperatures (800, 900, and 1000 °C) (Figure 1).

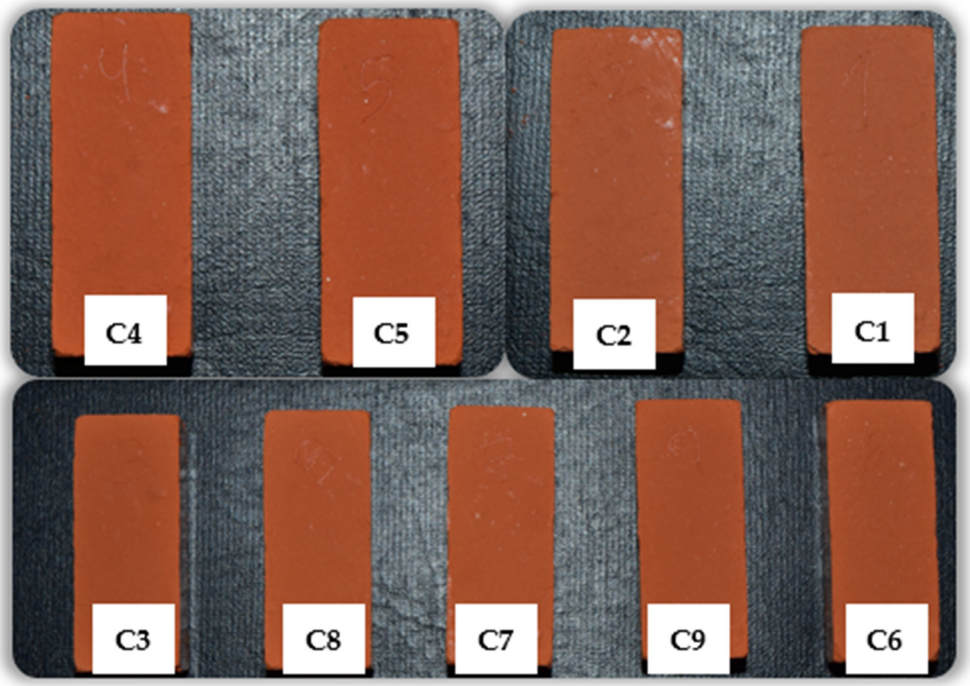

Figure 1. Specimens conformed according to Doehlert Design. Legend: C4 and C5: fired at 800 °C; C2 and C1: fired at 1000 °C; C3, C6, C7, C8 and C9: fired at 900 °C.

The selection of granite percentage and firing temperatures was guided by a Doehlert experimental matrix with two variables, including three replicates at the central point. The temperature parameters set were 800, 900, and 1000 °C, with granite powder proportions evaluated at 0, 5, 10, 20, and 30 wt%. The experimental design and conditions are summarized in Table 1, resulting in a total of nine experimental trials.

2.3.1. Water Absorption

This parameter was evaluated following an adaptation of the ASTM C20-00 standard [15], based on the relationship between the dry and wet weights of the specimens. The ceramic specimens were immersed in water for at least 24 h to obtain the wet weight. The wet weight was measured after the surface water was removed from the specimens.

2.3.2. Apparent Porosity

The apparent porosity of the specimens was determined by the ASTM C20-00 standard [15].

2.3.3. Compressive Strength

The compressive strength of the specimens was evaluated using a universal testing machine, model 300/15 kN, equipped with Servo-Plus Evolution control from MSTEST. The testing was conducted at a speed of 1 MPa/s, with an initial load of 1 N and a maximum load set to 30% of the specimen's capacity. The tests were carried out in the Concrete Laboratory of the School of Architecture at the Federal University of Pará (UFPA).

3. Results

3.1. Raw Materials

3.1.1. Mineralogical Composition

The XRD patterns of granite powder (GP-1) and the tailing sample (ALB-1) are shown in Figure 2. The granite powder is mainly composed of quartz, potassium feldspar, plagioclase, muscovite and kaolinite. Sample ALB-1 consists of kaolinite, gibbsite, Al-goethite, and hematite.

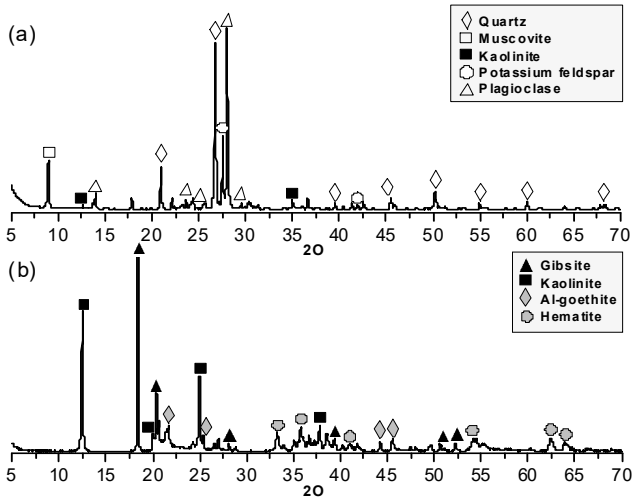

Figure 2. X-ray diffraction mineralogy patterns of GP-1 (**a**) and ALB-1 (**b**).

3.1.2. Chemical Composition

The chemical composition of the two samples is given in Table 2. Sample ALB-1 consists of Al_2O_3 (41.12%), SiO_2 (23%), and Fe_2O_3 (15.35%), while sample GP-1 consists of 74.4% SiO_2, 14.42% Al_2O_3, 4.45% K_2O and 3.86% Na_2O.

Table 2. Chemical composition of raw materials (wt%).

Sample	SiO_2	Al_2O_3	Fe_2O_3	TiO_2	K_2O	Na_2O	LOI	Other	Total
ALB-1	23	41.12	15.35	2.15	0.02	0.01	19.18	0.37	101.2
GRT-1	74.4	14.42	1.05	0.11	4.45	3.86	0.87	1.09	100.25

In sample ALB-1, the percentage of Al_2O_3 from the gibbsite and kaolinite domain, partial Al-goethite, SiO_2 from kaolinite, and Fe_2O_3 from goethite and hematite is reported. The percentage of SiO_2 in sample GP-1 is associated with silicates such as quartz, potassium feldspar, plagioclase, muscovite, and kaolinite.

The concentration of Al_2O_3 is associated with potassium feldspar, plagioclase, muscovite, and kaolinite. The percentage of K_2O is related to potassium feldspar, and the percentage of Na_2O is associated with plagioclase, probably albite.

3.1.3. Thermal Behavior

The thermal behavior of the samples can be seen in Figure 3. Sample ALB-1 shows three endothermic events in connection with mass loss (TG curve) and one exothermic event. In sample ALB-1, the first endothermic event at 293 °C is characteristic of the dehydroxylation of the mineral gibbsite; the event at 358 °C refers to the dehydroxylation of goethite, forming the mineral hematite; the third endothermic event at 510 °C is due to the loss of structural water from the mineral kaolinite [4]; and the exothermic event at 980 °C is characteristic of the formation of the mullite phase. Sample GP-1 showed no

significant mass loss (≈0.4%) and the DSC curve shows only one endothermic event at 576 °C. The endothermic event at 573 °C observed in sample GP-1 is due to the structural transformation of alpha quartz (α-SiO_2) into beta quartz (β-SiO_2) [16].

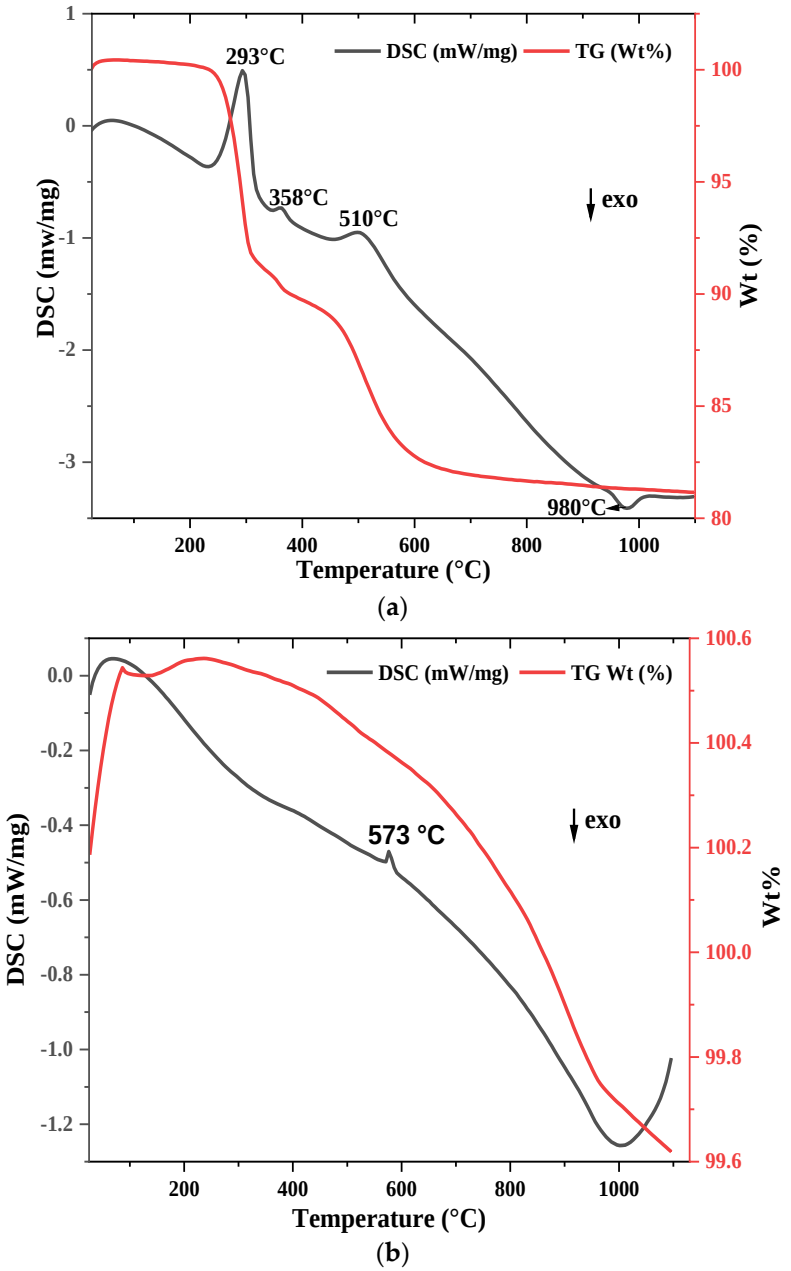

Figure 3. TG/DSC patterns of GP-1 (**a**) and ALB-1 (**b**). **Exo:** exothermic.

3.2. Fired Bricks (Specimens)

3.2.1. Mineralogical Composition

The composition of the specimens is shown in Figure 4. Quartz, plagioclase, and potassium feldspar were identified in all diffractograms for all compositions with granite components (C3 is the only one that does not contain granite), even if they were more "broadened" compared to the fresh sample (plagioclase and feldspar). Another mineral that was "preserved" during firing was hematite, which was present in all compositions.

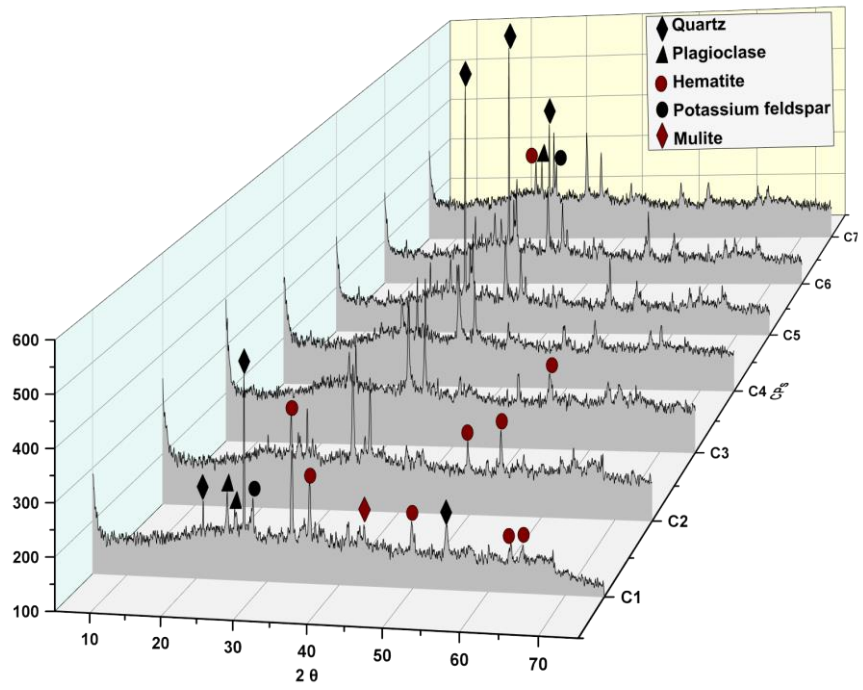

Figure 4. X-ray diffraction patterns of specimens (C1, C2, C3, C4, C5, C6 and C7).

The kaolinite, muscovite, gibbsite, and Al-goethite minerals present in the raw samples collapsed during firing. Most of the kaolinite may have given rise to amorphous materials (metakaolinite) or been transformed into mullite [3], as shown by the small peaks in the samples fired at 900 and 1000 °C.

3.2.2. Linear Firing Shrinkage (RLq)

The linear shrinkage of the test specimens (CP) is shown in Table 3. The values of the linear shrinkage are in the range of 1.19–3.71%. All the values are below the maximum allowed (8.0%) for good-quality bricks [17]. Linear shrinkage can be used as an indication of crack formation during the firing process of fired bricks [17,18].

Table 3. Linear retraction of the specimen (%).

Experiment	Dry Length	Length After Calcination	Linear Shrinkage (%)
C1	51.82	50.55	2.51
C2	51.81	50.24	3.13
C3	51.93	50.07	3.71
C4	51.79	50.96	1.63
C5	51.79	51.18	1.19
C6	51.93	51.23	1.37
C7	51.78	50.68	2.15 ± 0.25

3.2.3. Water Absorption and Apparent Porosity

Figure 5 illustrates the results of water absorption and apparent porosity. Water absorption is a fundamental parameter that indicates the potential of ceramic materials [19,20]. The highest apparent porosity value (72%) was obtained in experiment 3 (0% granite and 900 °C temperature) and the lowest values (60.7 and 60.2%) were observed in experiments 5 (20% granite and 900 °C temperature) and 6 (20% granite and 900 °C temperature), respectively. Regarding the water absorption results, the highest value was observed in experiment 3 (23.6%) and the lowest in experiment 6 (19.7%).

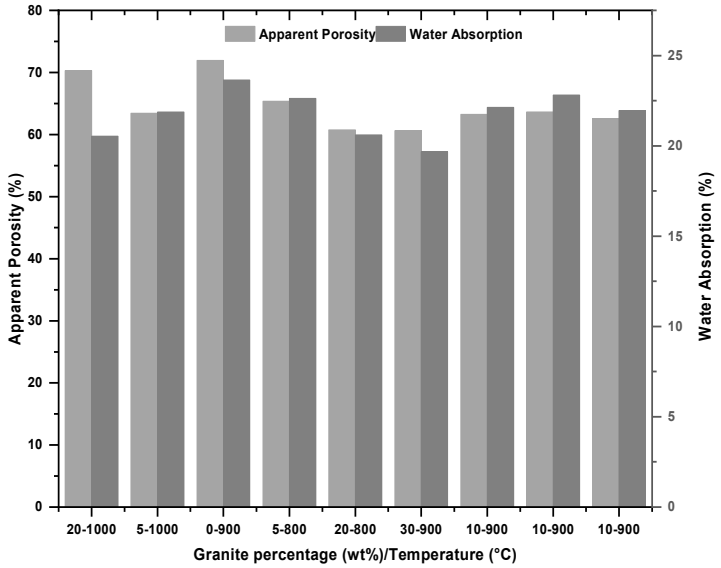

Figure 5. Apparent porosity and water absorption of specimens.

3.2.4. Compressive Strength

Figure 6 shows the results of the compressive strength of the specimen's compositions tested. The lowest results were obtained at 1000 °C (4.6 and 5.3 MPa) with a granite percentage of 20 and 6%, respectively. The best results were obtained at 900 °C without the addition of granite (11.9 MPa) and at 800 °C with the addition of 6% (14.9 MPa) and 20% granite (10.1 MPa). The standard deviation of the experiments was evaluated by the replicates of compositions 7 (6.43 MPa), 8 (7.14 MPa), and 9 (6.13 MPa) with an average of 6.55 ± 0.49 MPa. All the compressive strength results are above the values established by the ABNT and ASTM C55-17 standards [15,21–23].

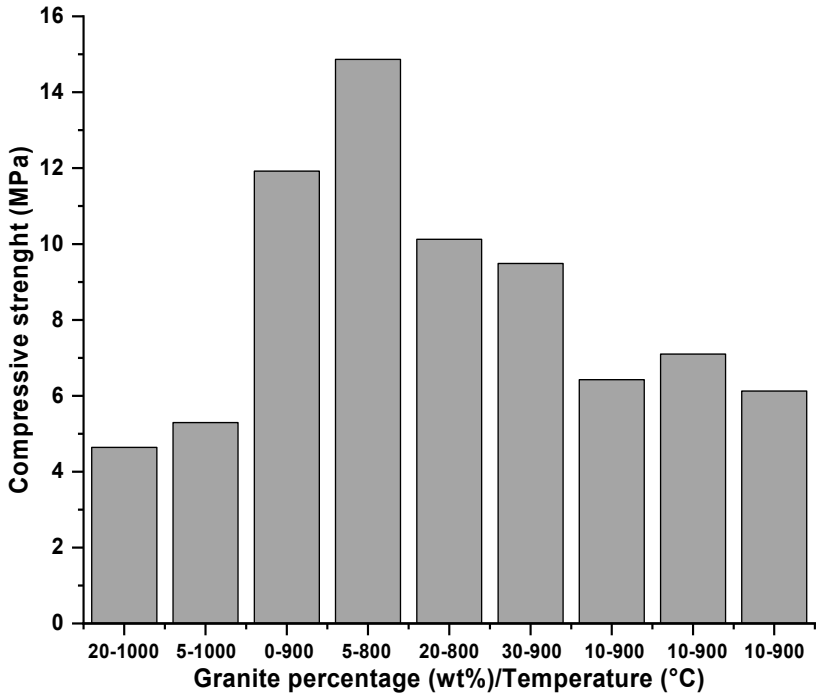

Figure 6. Compressive strength of specimens.

4. Discussion

4.1. Raw Materials

4.1.1. Mineralogical Composition and Chemical Composition

While kaolinite is one of the most important minerals used to produce ceramic materials, as it imparts plasticity to the ceramic body and contributes to resistance after firing [24,25], iron oxide minerals (Al-goethite and hematite) impart a reddish color; during firing, Al-goethite transforms into hematite. The contribution of kaolinite for ceramic is also described by [7]. The minerals in GP-1, mainly potassium feldspar, plagioclase, and muscovite, will mix to reduce porosity during the heating of the ceramic masses due to the presence of alkali metals, which will undergo a melting process [7,17].

The chemical composition of the samples, which is determined by the minerals present, has a direct effect on the technological properties of the ceramic product [1]. The presence of Al_2O_3, SiO_2, K_2O, and Fe_2O_3 in appropriate proportions is essential for establishing good properties in ceramic pieces [7].

4.1.2. Thermal Behavior

The events observed in sample ALB-1, which are associated with the loss of water forming the minerals gibbsite, goethite, and kaolinite, contribute to the formation of cracks during the heating of CPs produced only with this sample. On the other hand, no volatiles are observed in the granite sample. Due to this behavior, adding percentages of GP-1 to CPs with ALB-1 helps to reduce cracking during heating.

4.2. Specimens

4.2.1. Mineralogical Composition

Muscovite may have initiated its fusion process and contributed to the formation of a liquid phase during firing, thus enhancing the strength of the ceramic pieces. This behavior is essential to ensure suitable technological properties for ceramics. Other authors have already highlighted this characteristic [7].

The mineral gibbsite collapses and forms non-crystalline Al_2O_3, resulting in the refractory nature of the ceramic pieces. Al-goethite transforms into hematite, further accentuating the reddish color of the ceramic pieces.

4.2.2. Linear Firing Shrinkage (RLq)

The highest linear shrinkage value was obtained in CP-3, which was expected due to the predominance of kaolinite in the ALB-1 sample. The lowest linear shrinkage values were found in CP-5 (1.19%) and CP-6 (1.37%), which contain 30% and 20% granite, respectively. The higher value for CP-6 is due to the higher firing temperature (900 °C) than CP-5 (800 °C). These low linear shrinkage values are a consequence of the chemical/mineralogical composition of the granite, which contributes to reducing the plasticity of the CPs. This behavior was also identified by [7], who attributed the high linear shrinkage to the presence of kaolinite, while the reduced linear shrinkage was influenced by the presence of muscovite and other minerals that contribute to the formation of a liquid phase.

4.2.3. Water Absorption and Apparent Porosity

The results show a direct correlation between apparent porosity and water absorption, with the higher percentage of porosity directly influencing greater water absorption in the compositions studied. Although the incorporation of granite contributes to the formation of cracks and consequently to greater water absorption [15], its incorporation into the compositions studied reduced water absorption compared to the ceramic mass with only bauxite washing clay (experiment 3). The results are close to the maximum values allowed

by the standards (ABNT 15270-3, 2005a; ABNT 15310, 2005b) for ceramic bricks (≤20%) and tiles (≤22%) [21,23].

The increase in temperature contributed to the formation of greater porosity in the specimens fired at 900 and 1000 °C [2]. On the other hand, when the same temperature is analyzed with different percentages of granite, it is evident that the addition of granite favored a reduction in porosity and consequently a reduction in water absorption. All points mentioned are influenced by the predominance of kaolinite in the ALB-1 sample and the addition of the liquid phase from GP-1, as similarly defined by [7].

4.2.4. Compressive Strength

The temperature and percentage of granite directly influenced the gain and loss of resistance. At 800 °C, the sintering process was most effective in increasing resistance compared to 900 and 1000 °C. This behavior suggests that the release of volatile species during heating may have contributed to the formation of cracks, reducing the strength of the specimens at higher temperatures (900 and 1000 °C). A similar behavior was reported by [7], where higher temperatures decreased the strength of the specimens. Concerning the percentage of granite, it is clear that the addition of a low percentage was more favorable for gaining strength, but this gain was not as pronounced when compared to the strength value obtained with the ABT-1 sample alone. These characteristics suggest that the addition of a low percentage of granite contributes to reducing the plasticity of the ABT-1 sample and with the possible formation of a liquid phase after 900 °C, which contribute to a gain in strength, but that the percentage of granite above 10% may have reduced the plasticity to levels that jeopardize the strength of the ceramic mass [16,18,26].

5. Conclusions

The ALB sample (bauxite tailing) exhibits a composition similar to that of raw materials commonly used in the production of fired bricks, primarily due to the presence of minerals such as kaolinite and hematite. Additional minerals found in the sample, including gibbsite and Al-goethite, also contribute to the final properties of the bricks.

The technological properties of the bricks were directly influenced by the studied compositions. In terms of linear shrinkage, the addition of 20% and 30% granite resulted in the lowest shrinkage values, measuring 1.19% and 1.37%, respectively. Regarding apparent porosity, the incorporation of 20% granite at 900 °C yielded the lowest porosity values (60.7% and 60.2%), while the highest porosity was observed in specimens without granite. As for water absorption, all compositions complied with the requirements defined by relevant standards. In terms of compressive strength, granite additions ranging from 6% to 20% yielded satisfactory results, with compressive strengths of 14.9 MPa and 10.1 MPa, respectively. Although the incorporation of granite improved the ceramic properties, even the specimens without granite exhibited favorable characteristics, particularly in compressive strength (11.9 MPa). However, their water absorption exceeded the limits established by the ABNT standard.

The addition of granite powder partially altered the properties of the fired bricks. The incorporation of 6% granite powder proved to be the most beneficial, improving both water absorption and compressive strength. Thus, considering the overall characteristics of the ALB sample, its use in fired brick production—enhanced with granite powder as an additive—is technically feasible. This approach may contribute to reducing porosity and increasing mechanical strength in the final product.

The application of fired bricks presents a promising alternative for the reuse of bauxite tailings due to several advantages: fired brick manufacturing is a low-cost process, does

not require environmentally harmful additives, and enables the complete utilization of raw materials without generating additional waste post production.

Nonetheless, further investigation into the use of alternative additives is recommended to better understand their influence on red ceramics formulated with bauxite tailings, especially considering that variations in granite content and firing temperatures were not explored in this study.

Author Contributions: I.A.R.B.: Conceptualization, Methodology, Validation, Investigation, Formal analysis, Data curation, Writing—original draft, Writing—review & editing, Visualization; M.L.d.C.: Conceptualization, Methodology, Investigation, Writing—review & editing, Visualization, Funding acquisition, Project administration. All authors have read and agreed to the published version of the manuscript.

Funding: This research was supported by Hydro Company and the Dean of Research and Graduate Studies (PROPESP) of the Universidade Federal do Pará (UFPA).

Data Availability Statement: Data is contained within the article.

Acknowledgments: We thank the Hydro Company for providing the raw materials used in this study and financial support with the fieldwork.

Conflicts of Interest: The authors declare no conflict of interest. The funders had no role in the design of the study; in the collection, analyses, or interpretation of data; in the writing of the manuscript; or in the decision to publish the results.

References

1. Bai, M.; Xiao, J.; Gao, Q.; Shen, J. Utilization of Construction Spoil and Recycled Powder in Fired Bricks. *Case Stud. Constr. Mater.* **2023**, *18*, e02024. [CrossRef]
2. Sarani, N.A.; Kadir, A.A.; Din, M.F.M.; Amiza Hashim, A.; Hassan, M.I.H.; Hamid, N.J.A.; Hashar, N.N.H.; Hissham, N.F.N.; Johan, S.F.S.M. Physical-Mechanical Properties and Thermogravimetric Analysis of Fired Clay Brick Incorporating Palm Kernel Shell for Alternative Raw Materials. *Constr. Build. Mater.* **2023**, *376*, 131032. [CrossRef]
3. Wang, S.; Gainey, L.; Mackinnon, I.D.R.; Allen, C.; Gu, Y.; Xi, Y. Thermal Behaviors of Clay Minerals as Key Components and Additives for Fired Brick Properties: A Review. *J. Build. Eng.* **2023**, *66*, 105802. [CrossRef]
4. Adazabra, A.N.; Viruthagiri, G.; Yirijor, J. Combined Effects of Biomass Bottom Ashes and Spent Charcoal on Characteristics of Fired Clay Bricks. *Constr. Build. Mater.* **2023**, *399*, 132570. [CrossRef]
5. Makrygiannis, I.; Karalis, K. Optimizing Building Thermal Insulation: The Impact of Brick Geometry and Thermal Coefficient on Energy Efficiency and Comfort. *Ceramics* **2023**, *6*, 1449–1466. [CrossRef]
6. Makrygiannis, I.; Tsetsekou, A.; Papastratis, O.; Karalis, K. Assessing the Effects of Refuse-Derived Fuel (RDF) Incorporation on the Extrusion and Drying Behavior of Brick Mixtures. *Ceramics* **2023**, *6*, 2367–2385. [CrossRef]
7. Gadioli, M.C.B.; de Aguiar, M.C.; Vidal, F.W.H.; Sant'Ana, M.A.K.; de Almeida, K.M.; Giori, A.J.N. Incorporation of Ornamental Stone Waste in the Manufacturing of Red Ceramics. *Materials* **2022**, *15*, 5635. [CrossRef] [PubMed]
8. Kedziora, S.; Decker, T.; Museyibov, E.; Morbach, J.; Hohmann, S.; Huwer, A.; Wahl, M. Strength Properties of 316L and 17-4 PH Stainless Steel Produced with Additive Manufacturing. *Materials* **2022**, *15*, 6278. [CrossRef]
9. Gonçalves, R.M.; Martinho, A.; Oliveira, J.P. Recycling of Reinforced Glass Fibers Waste: Current Status. *Materials* **2022**, *15*, 1596. [CrossRef]
10. Badini, S.; Regondi, S.; Pugliese, R. Unleashing the Power of Artificial Intelligence in Materials Design. *Materials* **2023**, *16*, 5927. [CrossRef]
11. Freeland, B.; McCarthy, E.; Balakrishnan, R.; Fahy, S.; Boland, A.; Rochfort, K.D.; Dabros, M.; Marti, R.; Kelleher, S.M.; Gaughran, J. A Review of Polylactic Acid as a Replacement Material for Single-Use Laboratory Components. *Materials* **2022**, *15*, 2989. [CrossRef] [PubMed]
12. Bellucci, D.; Cannillo, V. Low-Temperature Sintering of a New Bioactive Glass Enriched with Magnesium Oxide and Strontium Oxide. *Materials* **2022**, *15*, 6263. [CrossRef]
13. Balti, S.; Boudenne, A.; Yahya, K.; Hamdi, N. Advancing Reinforcement of Sustainable Gypsum Composites: High-Performance Design by Reusing Waste Materials. *Mater. Today Sustain.* **2024**, *27*, 100946. [CrossRef]
14. Negrão, L.B.A.; da Costa, M.L.; Pöllmann, H. Waste Clay from Bauxite Beneficiation to Produce Calcium Sulphoaluminate Eco-Cements. *Constr. Build. Mater.* **2022**, *340*, 127703. [CrossRef]

15. Dong, Y.; Guo, W.; Jiang, C.; Shao, Y.; Zhang, L.; Wang, D.; Lu, X.; Huang, S.; Cheng, X. Using CaO as a Modifier Agent to Optimize the Pore Structure of Foamed Ceramics from Granite Scrap. *Ceram. Int.* **2023**, *49*, 13443–13451. [CrossRef]
16. Adazabra, A.N.; Viruthagiri, G.; Atingabono, J. Developing Fired Clay Bricks by Incorporating Scrap Incinerated Waste and River Dredged Sediment. *Process Saf. Environ. Prot.* **2023**, *179*, 108–123. [CrossRef]
17. Adazabra, A.N.; Viruthagiri, G. Effect of Variegated Biosolids Incorporation on the Technological Properties of Fired Clay Bricks Using Taguchi Method. *Case Stud. Constr. Mater.* **2023**, *19*, e02314. [CrossRef]
18. Wahab, R.A.A.; Mohammad, M.; Mazlan, M.; Yaki, A.N.A.; Bahari, N.S.S.; Fadzli, S.N.A.M.; Zahanis, Z.H.B.; Zaid, M.H.M. Study on the Physical and Mechanical Properties of Low Energy Consumption Fired Industrial Waste Clay Bricks from Eggshells and Rice Husks. *Mater. Today Proc.* **2023**, *75*, 79–83. [CrossRef]
19. Mohammad, M.; Abdul Wahab, R.A.; Mazlan, M.; Nisa Syuhaidah Mohamad Fazil, N.; Suraya Hanim Ibrahim, N.; Najiha Muhamad Nizam, U.; Humaidi Abu Hanifah, A.; Hafiz Mohd Zaid, M. Physical and Mechanical Properties of Fired Industrial Waste-Clay Bricks from Clam Shells and Soda Lime Silica Glass. In *Materials Today: Proceedings*; Elsevier Ltd.: Amsterdam, The Netherlands, 2022; Volume 75, pp. 151–155.
20. ABNT—Associação Brasileira de Normas Técnicas. *Alvenaria Estrutural—Blocos Cerâmicos Parte 3: Métodos de Ensaio*; Associação Brasileira de Normas Técnicas: Rio de Janeiro, RJ, Brazil, 2017; Volume 34.
21. ABNT—Associação Brasileira de Normas Técnicas. *NBR 15270-1: Componentes Cerâmicos. Parte 1: Blocos Cerâmicos Para Alvenaria de Vedação—Terminologia e Requisitos*; Associação Brasileira de Normas Técnicas: Rio de Janeiro, RJ, Brazil, 2005; Volume 15.
22. ABNT—Associação Brasileira de Normas Técnicas. *NBR 15270-2: Componentes Cerâmicos Parte 2: Blocos Cerâmicos Para Alvenaria Estrutural—Terminologia e Requisitos*; Associação Brasileira de Normas Técnicas: Rio de Janeiro, RJ, Brazil, 2017; Volume 15.
23. *ASTM C20-00*; Standard Test Methods for Apparent Porosity, Water Absorption, Apparent Specific Gravity, and Bulk Density of Burned Refractory Brick and Shapes by Boiling Water. American Society for Testing and Materials: West Conshohocken, PA, USA, 2015; pp. 1–3. [CrossRef]
24. Adazabra, A.N.; Viruthagiri, G.; Foli, B.Y. Evaluating the Technological Properties of Fired Clay Bricks Incorporated with Palm Kernel Shell. *J. Build. Eng.* **2023**, *72*, 106673. [CrossRef]
25. Zhao, J.; Wang, W.; Luan, Z.; He, M. First-Principles Analysis on Phase Transition, Atomic, Electronic, and Mechanical Properties of Kaolinite under Pressures. *Phys. B Condens. Matter.* **2024**, *674*, 415554. [CrossRef]
26. Pacheco, G.R.C.; Gonçalves, G.E.; Lins, V. de F.C. Design of Magnesia–Spinel Bricks for Improved Coating Adherence in Cement Rotary Kilns. *Ceramics* **2021**, *4*, 652–666. [CrossRef]